+1748 to +1860 containing the MRE125b in the human VDR mRNA was amplified by PCR using the following primers adapted to the *Xba*I site: 5'-TTT TCT AGA CTG CCT AAG TGG CTG CTG AC-3' and 5'-TTT TCT AGA CGC TGG ACA AGC GGG GCC-3'. The PCR product was digested with *Xba*I and the 119-bp fragment was cloned into pGL3-promoter vector, resulting in single (pGL3/F1) and reverse single (pGL3/R1) insertions. The fragment containing three copies of the MRE125b, 5'-CTA GA*C AGG AGA AAT GCA TCC ATT CCT CAG GGA* CAG AG*C AGG AGA AAT GCA TCC ATT CCT CAG GGA* CAG AG*C AGG AGA AAT GCA TCC ATT CCT CAG GGA* CAG AGT-3' (MRE125b is italicized), was cloned into the pGL3-promoter vector (pGL3/3xMRE). The complementary sequence of three copies of the MRE125b was also cloned into the pGL3-promoter plasmid (pGL3/3xMRE-Rev). A fragment containing the perfect matching sequence with the mature miR-125b, 5'-CTA GA*T CAC AAG TTA GGG TCT CAG GGA* T -3' (the matching sequence of miR-125b is italicized), was cloned into the pGL3-promoter vector (pGL3/c-125b). The nucleotide sequences of the constructed plasmids were confirmed by DNA sequencing analyses.

Luciferase assay

Various luciferase reporter plasmids (pGL3) were transiently transfected with phRL-TK plasmid into MCF-7 and KGN cells. Briefly, the day before transfection, the cells were seeded into 24-well plates. After 24 hr, 450 ng of pGL3 plasmid, 50 ng of phRL-TK plasmid and the precursors for miR-125b or control were co-transfected into MCF-7 cells using LipofectAMINE 2000. For KGN cells, 450 ng of pGL3 plasmid, 50 ng of phRL-TK plasmid and the AsOs for miR-125b or control were co-transfected using LipofectAMINE 2000. After incubation for 48 hr, the cells were resuspended in passive lysis buffer and then the luciferase activity was measured with a luminometer (Wallac, Turku, Finland) using the dual-luciferase reporter assay system.

Transfection of precursor for miR-125b into MCF-7 cells and preparation of nuclear extract and total RNA

To investigate the effects of miR-125b on the expression level of VDR protein, 50 nM precursors for miR-125b or control were transfected into MCF-7 cells using LipofectAMINE RNAiMAX. After 72 hr, nuclear extract was prepared using NE-PER Nuclear and Cytoplasmic extraction reagents (Pierce, Rockford, IL) and total RNA was prepared using ISOGEN according to the manufacturer's protocols. The protein concentration in the nuclear extract was determined using Bradford protein assay reagent (Bio-Rad, Hercules, CA) with γ-globulin as a standard.

Electrophoretic mobility shift assays

Human VDR cDNA was amplified by PCR using cDNA from human normal kidney with the forward primer 5'-TCC TTC AGG GAT GGA GGC AAT GGC-3' and the reverse primer 5'-CTG TCC TAG TCA GGA GAT CTC ATT GCC-3'. The PCR fragment was cloned into the pT7Blue T-Vector. The nucleotide sequences of the constructed plasmids were confirmed by DNA sequencing analyses. Human RXRα expression vector (pGEM-3Z/hRXRα) was previously constructed.[17] Using these plasmids and the TNT T7 Quick Coupled Transcription/Translation System (Promega), human VDR and RXRα proteins were synthesized in vitro. The oligonucleotide containing VDRE, 5'-aag CAC ACC cgg TGA ACT ccg-3' (the hexamer half-sites are capitalized), was from the human *CYP24* promoter.[18] Double-stranded oligonucleotides were labeled with [γ-^{32}P]ATP using T4 polynucleotide kinase (TOYOBO) and purified by Microspin G-50 columns (GE Healthcare Bio-Sciences, Piscataway, NJ). The labeled probe (40 fmol, ~10,000 cpm) was applied to each binding reaction in 25 mM HEPES-KOH buffer (pH 7.9), 0.5 mM EDTA, 50 mM KCl, 10% glycerol, 0.5 mM dithiothreitol, 0.5 mM (*p*-amidinophenyl) methanesulfonyl fluoride, 2 μg of poly(dI-dC), and 2 μL of in vitro transcribed/translated proteins to a final reaction volume of 15μL. For supershift experiments, 0.2 μg of anti-VDR antibodies or 2 μg of anti-RXRα antibodies were preincubated with in vitro transcribed/translated proteins or the nuclear extract at room temperature for 30 min. The mixtures were incubated on ice for 15 min and then loaded on 4% acrylamide gels in 0.5× Tris-borate EDTA buffer. The gels were dried

and then the DNA-protein complexes were detected with a Fuji Bio-Imaging Anlyzer BAS 1000 (Fuji Film, Tokyo, Japan).

Real-time RT-PCR for CYP24

To investigate the effects of miR-125b on the induction of CYP24 mRNA by $1,25(OH)_2D_3$, 50 nM precursors for miR-125b or control were transfected into MCF-7 cells using LipofectAMINE RNAiMAX. After 72 hr, the cells were treated with 100 nM $1,25(OH)_2D_3$ (or 0.1% ethanol for control) for 24 hr. Total RNA was prepared using ISOGEN. The forward and reverse primers for CYP24 mRNA were 5'-CAG CAA ACA GTC TAA TGT GG-3' and 5'-AGC ATA TTC ACC CAG AAC TG-3', respectively. The real-time PCR analysis was performed as follows: after an initial denaturation at 95°C for 30 sec, the amplification was performed by denaturation at 94°C for 4 sec, annealing and extension at 62°C for 20 sec for 45 cycles. The CYP24 mRNA levels were normalized with GAPDH mRNA as described previously.[19]

Growth Assay

To investigate the effects of miR-125b on the anti-proliferative effects of $1,25(OH)_2D_3$, growth assay was conducted according to the method by McGaffin *et al.*[20] with slight modifications. MCF-7 cells were plated on 96 well plates (3000 cells/well) and 20 nM precursors for miR-125b or control were transfected using LipofectAMINE RNAiMAX. After 24 hr, the cells were treated with 1 μM $1,25(OH)_2D_3$ (or 0.1% ethanol) for 48-96 hr. The cells were rinsed with phosphate-buffered saline, fixed with 3.7% formaldehyde for 15 min, and stained with 0.1% crystal violet for 10 min. The stained cells were washed with water and air-dried. Crystal violet was extracted from the stained cells with 2% sodium dodecyl sulfate, and the intensities were quantified spectrophotometrically 620 nm. The percent cell viability was calculated by comparison with the absorbance of control cells.

Statistical analyses

Data are expressed as mean ± SD of triplicate determinations. Comparison of two groups was made with an unpaired, two-tailed student's *t* test. Comparison of multiple groups was made with ANOVA followed by Dunnett or Tukey test. A value of $P < 0.05$ was considered statistically significant.

Results

A miR-125b complementary sequence on the 3'-UTR of human VDR mRNA

By a computational search (http://www.targetscan.org/), several miRNAs are found to share complementarity with a sequence in the 3'-UTR of human VDR mRNA. Among them, we focused on miR-125b because its binding site is highly conserved among species (Fig. 1). The seed sequence of miR-125b was perfectly matching with the predicted binding site of the VDR mRNA. We investigated whether miR-125b might be involved in the regulation of human VDR expression through the MRE125b.

Expression levels of miR-125b in human cancer cell lines

For gain- and loss-of-function experiments, we need to know the expression level of endogenous miR-125b in cell lines. For this purpose, the expression levels of mature miR-125b in six kinds of human cancer cell lines were determined by real-time RT-PCR analysis. As shown in Fig. 2A, the mature miR-125b level was highest in KGN followed by MDA-MB-435 cells, whereas it was extremely low in MCF-7, HepG2, HEK293, and LS180 cells.

Effects of overexpression or inhibition of miR-125b on luciferase activity

To investigate whether MRE125b is functional in the regulation by miR-125b, luciferase assays were performed. First, we transfected the precursor for miR-125b into MCF-7 cells in which the mature miR-125b level was low (Fig. 2B). Using the pGL3/c-125b plasmid containing the miR-125b complementary sequence, it was demonstrated that the luciferase

activity was significantly ($P < 0.001$) decreased by the transfection of precursor for miR-125b. The luciferase activity of the pGL3/F1 plasmid was significantly ($P < 0.001$) decreased (60% of control) by the overexpression of miR-125b, but that of the pGL3/R1 plasmid was not. When the pGL3/3xMRE plasmid containing three copies of the MRE125b was used, a prominent suppression was observed (40% of control, $P < 0.001$) by the overexpression of miR-125b. Next, we transfected the AsO for miR-125b into KGN cells in which the mature miR-125b was highly expressed (Fig. 2B). The luciferase activity of the pGL3/c-125b plasmid was significantly ($P < 0.01$) lower than that of the control pGL3-p plasmid. The luciferase activity of the pGL3/c-125b plasmid was significantly ($P < 0.01$) restored by the transfection of AsO for miR-125b (3.1-fold of control). The luciferase activity of the pGL3/F1 plasmid was increased by the transfection of AsO for miR-125b, although the effects were statistically insignificant. The luciferase activity of the pGL3/3xMRE plasmid was significantly ($P < 0.01$) lower than that of the control pGL3-p plasmid. The luciferase activity of the pGL3/3xMRE plasmid was significantly (1.3-fold of control, $P < 0.05$) restored by the inhibition of miR-125b by AsO. These results suggest that miR-125b functionally recognized the MRE125b on the human VDR mRNA.

Effects of overexpression of miR-125b on the endogenous VDR protein level

We sought to examine the effects of miR-125b on the endogenous VDR protein level. When we first attempted to determine the endogenous VDR protein level in human cancer cell lines by Western blot analysis using commercially available antibodies, we could not identify the VDR protein because of multiple non-specific bands. Therefore, we utilized electrophoretic mobility shift assays to evaluate the endogenous VDR level. The VDRE of human *CYP24* gene, which is known to be a target of VDR,[18] was used as a probe. It was confirmed that in vitro-synthesized VDR/RXRα heterodimers bound to the VDRE (Fig. 3A). With the anti-VDR or anti-RXRα antibodies, the band density of the VDR/RXRα heterodimer was decreased and the super-shifted band was observed. When the probe was incubated with the nuclear extracts prepared from MCF-7 cells, the band representing the VDR/RXRα

heterodimer was observed and the band density was diminished with the anti-VDR or anti-RXRα antibodies. When the precursor for miR-125b was transfected, the mature miR-125b level was prominently increased, and the band density of the VDR/RXRα heterodimer was significantly ($P < 0.001$) decreased compared with that of control (40% of control). We confirmed by Western blot analysis that the expression level of RXRα was not affected by the overexpression of miR-125b (data not shown). These results suggest that the endogenous VDR level was repressed by miR-125b.

MiR-125b-dependent VDR regulation affects the target gene expression

We investigated whether the miR-125b-dependent regulation of VDR affects the expression of target genes. When the MCF-7 cells were treated with 100 nM $1,25(OH)_2D_3$, the CYP24 mRNA level was significantly ($P < 0.001$) increased (588-fold) (Fig. 4). However, this induction was markedly attenuated by the overexpression of miR-125b. In addition, the basal CYP24 mRNA level was also decreased by the overexpression of miR-125b, although it was statistically insignificant. These results support that the endogenous VDR level was repressed by miR-125b, and this regulation mechanism affects the expression of target genes.

Effects of overexpression of miR-125b on the anti-proliferative effects of $1,25(OH)_2D_3$

We investigated the effects of miR-125b on the anti-proliferative effects of $1,25(OH)_2D_3$ (Fig. 5). The cells transfected with the precursor for control were grown during incubation for 48-96 hr, but the growth was significantly ($P < 0.01$ or $P < 0.001$) reduced in the presence of 1 μM $1,25(OH)_2D_3$. Interestingly, the overexpression of miR-125b prominently ($P < 0.05$, $P < 0.01$ or $P < 0.001$) abolished the anti-proliferative effects of $1,25(OH)_2D_3$. In addition, the overexpression of miR-125b could significantly ($P < 0.05$, at 96 hr) increase the cell growth in the absence of $1,25(OH)_2D_3$. These results suggest that miR-125b regulating VDR has a great impact on anti-proliferative effects of $1,25(OH)_2D_3$.

Discussion

In the present study, we investigated whether human VDR might be regulated by miRNA. In the 3'-UTR of human VDR mRNA, a potential miR-125b recognition element (MRE125b) was identified. Luciferase assays clearly revealed that the miR-125b negatively regulated the reporter activity through MRE125b. By electrophoretic mobility shift assays and evaluation of the induction potencies of CYP24 mRNA, it was demonstrated that the endogenous VDR level was repressed by the overexpression of miR-125b. These results clearly suggest that the human VDR is post-transcriptionally regulated by miR-125b. Because the sequences of VDR mRNA around MRE125b are highly conserved among species (Fig. 1), the regulation by miR-125b may also occur in other species.

The global expression of miRNAs is deregulated in most cancer types.[21] Some studies have suggested that miRNA expression would be widely down-regulated in human tumors relative to normal tissues, and other studies reported a tumor-specific mixed pattern of down-regulation and up-regulation of miRNA genes. Recent findings revealed that the miRNA deregulation in human cancers occurs by multiple mechanisms, including transcriptional deregulation, epigenetic alterations, mutation, DNA copy number abnormalities, and dysfunction of key proteins in the miRNA biogenesis pathway.[21] Among them, alterations in DNA copy numbers would be a major mechanism because over 50% of miRNAs are in genomic fragile sites or regions associated with cancers.[12] It has been reported that miR-125b was down-regulated in breast[12,22] and prostate[23] cancers. Mature miR-125b is formed by two precursors, miR-125b-1 and miR-125b-2. The genes for miR-125b-1 and miR-125b-2 are located in chromosome 11q24.1 and 21q11.2, respectively (http://microrna.sanger.ac.uk/sequences/). Interestingly, it has been reported that the chromosome region 11q23-24 is most frequently deleted in breast, ovarian, and lung cancers[24,25] and the chromosome region 21q11-21 is frequently deleted in breast, esophagus, stomach, ovary, and lung cancers.[26] This could be one of the mechanisms of the down-regulation of miR-125b in cancers. Meanwhile, it is known that VDR is up-regulated in several cancers,[8,9] and the up-regulation appears to be associated with a good prognosis.[27]

Since the present study demonstrated that miR-125b negatively regulated the expression of VDR, it was directly proven that the up-regulation of VDR in cancers would be due to the down-regulation of miR-125b.

Previously, the role of miR-125b in cell proliferation and differentiation has been reported in human breast cancer cell lines,[28] thyroid carcinoma cells,[29] a bone marrow stroma cell line,[30] and hepatocellular carcinoma.[31] Scott *et al.*[32] reported that the miR-125b suppressed *ERBB2* and *ERBB3* oncogenes. Li *et al.*[31] reported that high expression of miR-125b was correlated with good survival in hepatocellular carcinoma patients. These previous studies suggest that miR-125b acts as a type of tumor suppressor gene. In contrast, our study demonstrated that miR-125b repressed the anti-proliferative effects of $1,25(OH)_2D_3$. Thus, the present study provides new information concerning the role of miR-125b in cell proliferation. In cancer cells, the down-regulation of miR-125b would result in an augmentation of the anti-tumor effects of $1,25(OH)_2D_3$.

As regards other nuclear receptors, there are a few reports. Estrogen receptor (ER) α, which is an important marker for the prognosis and is predictive of the response to endocrine therapy in breast cancer patients, has been found to be regulated by miR-206[33] and miR-221/222.[34] These studies suggested that these miRNAs could serve as potential therapeutic targets for a subset of ERα-negative breast cancers. Previously, we found that pregnane X receptor (PXR), which is a key regulator of the expression of drug-metabolizing enzymes and transporters involved in the responses to steroids and xenobiotics, is regulated by miR-148a.[35] Thus, accumulating evidence has revealed that nuclear receptors, to which steroid hormones bind as a ligand, are regulated by miRNAs. The regulation of nuclear receptors by miRNA would result in changes in the expression of a variety of target genes, constructing complex regulatory networks.

In conclusion, we clarified that human VDR is post-transcriptionally regulated by miR-125b. This study could provide new insights into the regulatory mechanism of VDR expression.

Acknowledgements

This work was supported in part by Health and Labor Science research grants from the Ministry of Health, Labor, and Welfare of Japan. We acknowledge Mr. Brent Bell for reviewing the manuscript.

References

1. Dusso AS, Brown AJ, Slatopolsky E. Vitamin D. Am J Physiol Renal Physiol 2005;289:F8-F28.
2. Nagpal S, Na S, Rathnachalam R. Noncalcemic actions of vitamin D receptor ligands. Endocr Rev 2005;26:662-87.
3. Holick MF. Vitamin D deficiency. N Engl J Med 2007;357:266-81.
4. Garland CF, Garland FC, Gorham ED, Lipkin M, Newmark H, Mohr SB, Holick MF. The role of vitamin D in cancer prevention. Am J Public Health 2006;96:252-61.
5. Carlberg C, Polly P. Gene regulation by vitamin D_3. Crit Rev Eukaryot Gene Expr 1998;8:19-42.
6. Zou A, Elgort MG, Allegretto EA. Retinoid X receptor (RXR) ligands activate the human 25-hydroxyvitamin D_3-24-hydroxylase promoter via RXR heterodimer binding to two vitamin D-responsive elements and elicit additive effects with 1,25-dihydroxyvitamin D_3. J Biol Chem 1997;272:19027-34.
7. Segura C, Alonso M, Fraga C, García-Caballero T, Diéguez C, Pérez-Fernández R. Vitamin D receptor ontogenesis in rat liver. Histochem Cell Biol 1999;112:163-7.
8. Friedrich M, Axt-Fliedner R, Villena-Heinsen C, Tilgen W, Schmidt W, Reichrath J. Analysis of vitamin D-receptor (VDR) and retinoid X-receptor α in breast cancer. Histochem J 2002;34:35-40.
9. Khadzkou K, Buchwald P, Westin G, Dralle H, Akerström G, Hellman P. 25-Hydroxyvitamin D_3 1α-hydroxylase and vitamin D receptor expression in papillary thyroid carcinoma. J Histochem Cytochem 2006;54:355-61.
10. Cross HS, Bareis P, Hofer H, Bischof MG, Bajna E, Kriwanek S, Bonner E, Peterlik M. 25-Hydroxyvitamin D_3-1α-hydroxylase and vitamin D receptor gene expression in human colonic mucosa is elevated during early cancerogenesis. Steroids 2001;66:287-92.
11. Ambros V. The functions of animal microRNAs. Nature 2004;431:350-5.

12. Calin GA, Sevignani C, Dumitru CD, Hyslop T, Noch E, Yendamuri S, Shimizu M, Rattan S, Bullrich F, Negrini M, Croce CM. Human microRNA genes are frequently located at fragile sites and genomic regions involved in cancers. Proc Natl Acad Sci USA 2004;101:2999-3004.

13. Lu J, Getz G, Miska EA, Alvarez-Saavedra E, Lamb J, Peck D, Sweet-Cordero A, Ebert BL, Mark RH, Ferrando AA, Downing JR, Jacks T, Horvitz HR, Golub TR. MicroRNA expression profiles classify human cancers. Nature 2005;435:834-8.

14. Bartel DP. MicroRNAs: genomics, biogenesis, mechanism, and function. Cell 2004;116:281-97.

15. Lewis BP, Burge CB, Bartel DP. Conserved seed pairing, often flanked by adenosines, indicates that thousands of human genes are microRNA targets. Cell 2005;120:15-20.

16. Nishi Y, Yanase T, Mu YM, Oba K, Ichino I, Saito M, Nomura M, Mukasa C, Okabe T, Goto K, Takayanagi R, Kashimura Y, Haji M, Nawata H. Establishment and characterization of a steroidogenic human granulosa-like tumor cell line, KGN, that expresses functional follicle-stimulating hormone receptor. Endocrinology 2001;142:437-45.

17. Itoh M, Nakajima M, Higashi E, Yoshida R, Nagata K, Yamazoe Y, Yokoi T. Induction of human CYP2A6 is mediated by the pregnane X receptor with peroxisome proliferator-activated receptor-γ coactivator 1α. J Pharmacol Exp Ther 2006;319:693-702.

18. Chen KS, DeLuca HF. Cloning of the human 1α,25-dihydroxyvitamin D-3 24-hydroxylase gene promoter and identification of two vitamin D-responsive elements. Biochim Biophys Acta 1995;1263:1-9.

19. Tsuchiya Y, Nakajima M, Kyo S, Kanaya T, Inoue M, Yokoi T. Human CYP1B1 is regulated by estradiol via estrogen receptor. Cancer Res 2004;64:3119-25.

20. McGaffin KR, Acktinson LE, Chrysogelos SA. Growth and EGFR regulation in breast cancer cells by vitamin D and retinoid compounds. Breast Cancer Res Treat 2004;86:55-73.

21. Deng S, Calin GA, Croce CM, Coukos G, Zhang L. Mechanisms of microRNA deregulation in human cancer. Cell Cycle 2008;7:2643-6.

22. Iorio MV, Ferracin M, Liu CG, Veronese A, Spizzo R, Sabbioni S, Magri E, Pedriali M, Fabbri M, Campiglio M, Menard S, Palazzo JP, Rosenberg A, Musiani P, Volinia S, Nenci I, Calin GA, Querzoli P, Negrini M, Croce CM. MicroRNA gene expression deregulation in human breast cancer. Cancer Res 2005;65:7065-70.

23. Ozen M, Creighton CJ, Ozdemir M, Ittmann M. Widespread deregulation of microRNA expression in human prostate cancer. Oncogene 2007;27:1788-93.

24. Negrini M, Rasio D, Hampton GM, Sabbioni S, Rattan S, Carter SL, Rosenberg AL, Schwartz GF, Shiloh Y, Cavenee WK, Croce CM. Definition and refinement of chromosome 11 regions of loss of heterozygosity in breast cancer: identification of a new region at 11q23.3. Cancer Res 1995;55:3003-7.

25. Rasio D, Negrini M, Manenti G, Dragani TA, Croce CM. Loss of heterozygosity at chromosome 11q in lung adenocarcinoma: identification of three independent regions. Cancer Res 1995;55:3988-91.

26. Yamada H, Yanagisawa K, Tokumaru S, Taguchi A, Nimura Y, Osada H, Nagino M, Takahashi T. Detailed characterization of a homozygously deleted region corresponding to a candidate tumor suppressor locus at 21q11-21 in human lung cancer. Genes Chromosomes Cancer 2008;47:810-8.

27. Seubwai W, Wongkham C, Puapairoj A, Khuntikeo N, Wongkham S. Overexpression of vitamin D receptor indicates a good prognosis for cholangiocarcinoma: implications for therapeutics. Cancer 2007;109:2497-505.

28. Lee YS, Kim HK, Chung S, Kim K-S, Dutta A. Depletion of human micro-RNA miR-125b reveals that it is critical for the proliferation of differentiated cells but not for the down-regulation of putative targets during differentiation. J Biol Chem 2005;280:16635-41.

29. Visone R, Pallante P, Vecchione A, Cirombella R, Ferracin M, Ferraro A, Volinica S, Coluzzi S, Leone V, Borbone E, Liu C-G, Petrocca F, Troncone G, Caalin GA, Scarpa A, Colato C, Tallini G, Santoro M, Croce CM, Fusco A. Specific microRNAs are downregulated in human thyroid anaplastic carcinomas. Oncogene 2007;26:7590-5.

30. Mizuno Y, Yagi K, Tokuzawa Y, Kanesaki-Yatsuka Y, Suda T, Katagiri T, Fukuda T, Maruyama M, Okuda A, Amemiya T, Kondoh Y, Tashiro H, Okazaki Y. MiR-125b inhibits osteoblastic differentiation by down-regulation of cell proliferation. Biochem Biophys Res Commun 2008;368:267-72.

31. Li W, Xie L, He X, Li J, Tu K, Wei L, Wu J, Guo Y, Ma X, Zhang P, Pan Z, Hu X, Zhao Y, Xie H, Jiang G, Chen T, Wang J, Zheng S, Cheng J, Wan D, Yang S, Li Y, Gu J. Diagnostic and prognostic implications of microRNAs in human hepatocellular carcinoma. Int J Cancer 2008;123:1616-22.

32. Scott GK, Goga A, Berger C, Sullivan CS, Benz CC. Coordinate suppression of ERBB2 and ERBB3 by enforced expression of micro-RNA miR-125a or miR-125b. J Biol Chem 2007;282:1479-86.

33. Adams BD, Furneaux H, White BA. The micro-ribonucleic acid (miRNA) miR-206 targets the human estrogen receptor-α (ERα) and represses ERα messenger RNA and protein expression in breast cancer cell lines. Mol Endocrinol 2007;21:1132-47.

34. Zhao JJ, Lin J, Yang H, Kong W, He L, Ma X, Coppola D, Cheng JQ. MicroRNA-221/222 negatively regulates ERα and associates with tamoxifen resistance in breast cancer. J Biol Chem 2008;283:31079-86.

35. Takagi S, Nakajima M, Mohri T, Yokoi T. Post-transcriptional regulation of human pregnane X receptor by micro-RNA affects the expression of cytochrome P450 3A4. J Biol Chem 2008;283:9674-80.

Figure legends

FIGURE 1. Schematic representation of human VDR mRNA and the predicted target sequence of miR-125b. The numbering refers to the 5' end of mRNA as 1, and the coding region is from +161 to +1444. MRE125b is located on +1786 to +1813 in the 3'-UTR of human VDR mRNA. Gray box, highly conserved regions. *bold letters*, seed sequence.

FIGURE 2. Expression levels of mature miR-125b in various human cell lines and luciferase assays in MCF-7 and KGN cells. (*a*) The expression levels of mature miR-125b in MCF-7, MDA-MB-435, KGN, HepG2, HEK293, and LS180 cells were determined by real-time RT-PCR analysis using an NCode miRNA first-strand cDNA synthesis kit. The values were the mature miR-125b levels relative to those in MCF-7 cells. (*b*) Luciferase assays were performed to investigate whether MRE125b is functional in the regulation by miR-125b. A series of reporter constructs was transiently transfected with 10 pmol precursors for miR-125b or control into 5 x 10^4 MCF-7 cells, or with 5 pmol AsO for miR-125b or control into 8 x 10^4 KGN cells. The firefly luciferase activity for each construct was normalized with the *Renilla* luciferase activities. Values are expressed as percentages of the relative luciferase activity of pGL3-promoter plasmid. Each column represents the mean ± SD of three independent experiments. $*P < 0.05$, $**P < 0.01$, $*** P < 0.001$, compared with the precursor or AsO for control. †† $P < 0.01$, compared with pGL3-p.

FIGURE 3. Electrophoretic mobility shift assays to evaluate the endogenous VDR protein level. (*a*) Electrophoretic mobility shift assays were performed with oligonucleotide probe containing the VDRE in the human CYP24 promoter. The ^{32}P labeled probe was incubated with in vitro-synthesized VDR (rVDR) and RXRα (rRXRα) or the nuclear extract prepared from the precursors for miR-125b or control-transfected MCF-7 cells. For supershift analysis, 0.2 μg of anti-VDR antibodies (αVDR) or 2 μg of anti-RXRα antibodies (αRXRα) were pre-incubated with in vitro-synthesized proteins or the nuclear extract at room temperature for

30 min. The lower arrow indicates the VDR/RXRα-dependent shifted band and the upper arrow indicates the supershifted (SS) complex. (*b*) The mature miR-125b level was determined by real-time RT-PCR analysis. Total RNA was prepared from MCF-7 cells 72 hr after the transfection of the precursors for miR-125b or control (50 nM). The values are the mature miR-125b levels normalized with the U6 snRNA levels relative to control. (*c*) The relative density of the shifted band including VDR/RXRα complex. Each column represents the mean ± SD of three independent experiments. ***$P < 0.001$, compared with the precursor for control.

FIGURE 4. Induction of CYP24 mRNA in MCF-7 cells by $1,25(OH)_2D_3$. The precursors for miR-125b or control (50 nM) were transfected into MCF-7 cells. After 72 hr, the cells were treated with 100 nM $1,25(OH)_2D_3$ or 0.1% ethanol (vehicle) for 24 hr and then total RNA was prepared. The CYP24 mRNA levels were determined by real-time RT-PCR and normalized with the GAPDH mRNA level. The data are expressed relative to the CYP24 mRNA level in the precursor for control-transfected cells in the absence of $1,25(OH)_2D_3$. Each column represents the mean ± SD of three independent experiments. *$P < 0.05$; ***$P < 0.001$.

FIGURE 5. Anti-proliferative effects of $1,25(OH)_2D_3$ in MCF-7 cells. The precursors for miR-125b or control (20 nM) were transfected into MCF-7 cells. After 24 hr, the cells were treated with 1 μM $1,25(OH)_2D_3$ or 0.1% ethanol (vehicle) for 48-96 hr and then crystal violet assays were performed. Values are expressed as percentages change in growth relative to the cell viability in the precursor for control-transfected cells in the absence of $1,25(OH)_2D_3$ after 48 hr incubation. Each point represents the mean ± SD of three independent experiments. *$P < 0.05$, **$P < 0.01$, *** $P < 0.001$, compared with the vehicle. †$P < 0.05$, ††$P < 0.01$, ††† $P < 0.001$, compared with the precursor for control.

Fig. 1. Mohri *et al.*

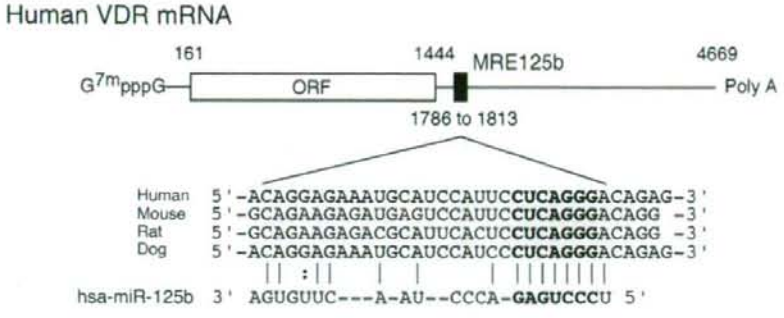

160x80mm (600 x 600 DPI)

Fig. 2. Mohri *et al.*

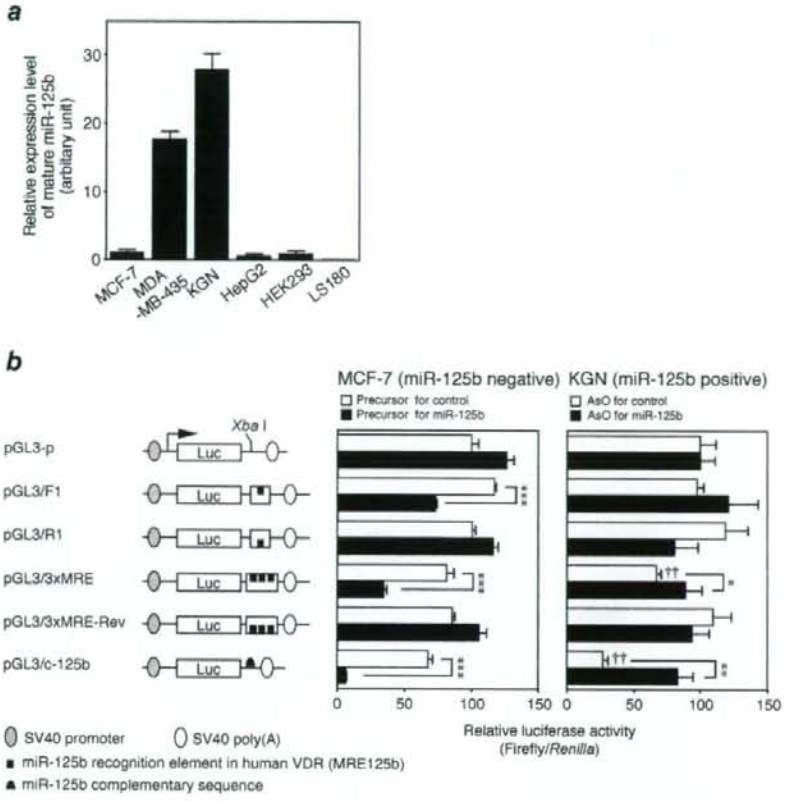

180x190mm (600 x 600 DPI)

Fig. 3. Mohri *et al.*

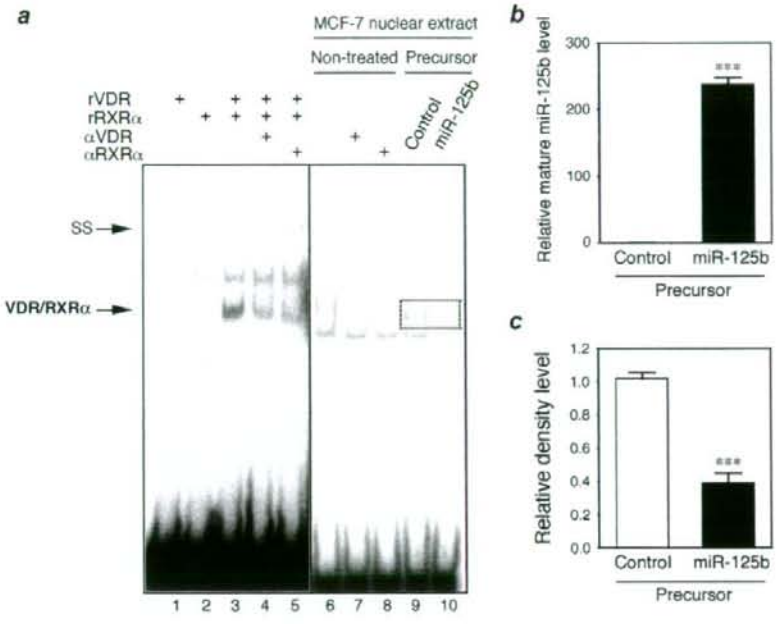

180x166mm (600 x 600 DPI)

Fig. 4. Mohri *et al.*

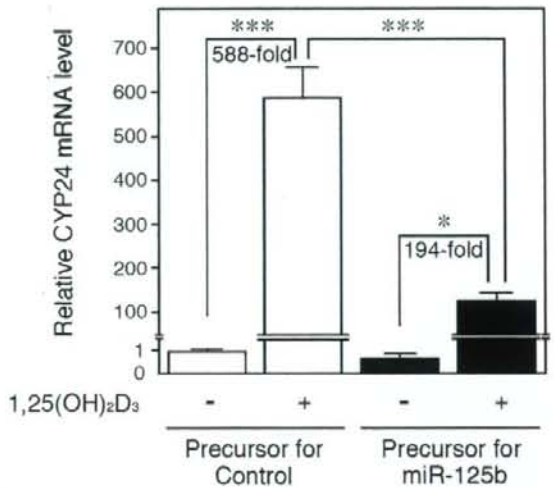

115x87mm (600 x 600 DPI)

Fig. 5. Mohri *et al.*

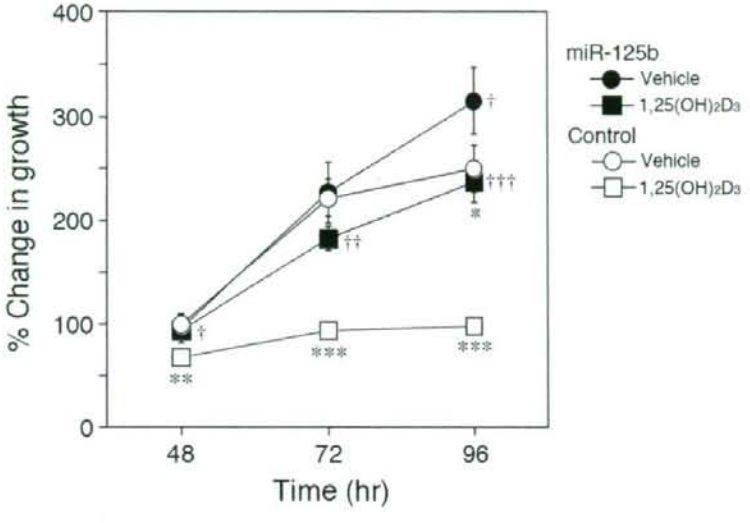

120x91mm (600 x 600 DPI)